

SPECTROSCOPY DETERMINATION OF METFORMIN IN DRINKING WATER, TABLET, HUMAN SERUM, AND URINE BASED ON THE AGGREGATION OF NANOPARTICLES**M. Moradi, M. R. Sohrabi*, S. Mortazavinik**

Department of Chemistry, North Tehran Branch at Islamic Azad University,
Tehran, Iran; e-mail: sohrabi.m46@yahoo.com

Simple, rapid, and sensitive ultraviolet-visible spectroscopy method was used to determine ultra-trace amounts of metformin (MET) in several samples such as drinking water, tablet, serum (blood), and urine without preconcentration step. Gold nanoparticles (AuNPs) were synthesized, and determination of MET was carried out based on the surface plasmon resonance property of AuNPs and the interaction between MET and AuNPs. Transmission electron microscopy (TEM) was utilized to characterize the structure of AuNPs before and after addition MET. Also, dynamic light scattering was used to investigate the size of nanoparticles distribution. The results showed that AuNPs were aggregated in the presence of the MET. Some parameters, including pH, AuNPs concentration, contact time, buffers, and ionic strength, were evaluated to select optimum conditions. Linear range obtained was 15–300 $\mu\text{g/L}$ in the optimum conditions. Also, the correlation coefficient (R^2), the limit of detection, and limit of quantification were equal to 0.9918, 0.99, and 1.12 $\mu\text{g/L}$, respectively. In addition, the effect of interfering species was investigated. Finally, the results of the analysis of different real samples indicated that the proposed method was suitable and accurate for determination of MET.

Keywords: spectroscopy, ultra-trace, metformin, gold nanoparticles, surface plasmon resonance, real samples.

СПЕКТРОСКОПИЧЕСКОЕ ОПРЕДЕЛЕНИЕ МЕТФОРМИНА В ПИТЬЕВОЙ ВОДЕ, ТАБЛЕТКАХ, СЫВОРОТКЕ КРОВИ И УРИНЕ ЧЕЛОВЕКА НА ОСНОВЕ АГРЕГАЦИИ НАНОЧАСТИЦ

УДК 543.42:620.3

M. Moradi, M. R. Sohrabi*, S. Mortazavinik

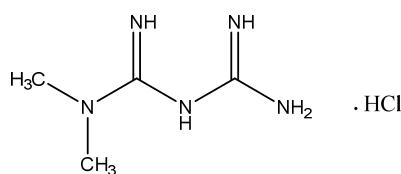
Северо-Тегеранский филиал Исламского университета Азад,
Тегеран, Иран; e-mail: sohrabi.m46@yahoo.com

(Поступила 5 июля 2019)

Простой, быстрый и чувствительный метод УФ-видимой спектроскопии использован для определения предельно малых количеств метформина (MET) в питьевой воде, таблетках, сыворотке крови и урине человека без стадии предварительного концентрирования. Синтезированы наночастицы золота (AuNPs). Определение MET проводилось на основе поверхностного плазмонного резонанса на частицах AuNPs и данных о взаимодействии между MET и AuNPs. Для анализа структуры AuNPs до и после добавления MET использована просвечивающая электронная микроскопия. Распределение наночастиц по размерам исследовано с помощью динамического рассеяния света. Результаты показывают, что в присутствии MET происходит агрегация AuNPs. Ряд параметров, включая pH, концентрацию AuNPs, время контакта, ионную силу, а также влияние буфера оценены для выбора оптимальных условий. В оптимальных условиях линейный диапазон 15–300 мкг/л. Коэффициент корреляции (R^2), предел обнаружения и предел количественной оценки равны 0.9918, 0.99 и 1.12 мкг/л соответственно. Исследовано влияние мешающих веществ. Предлагаемый метод пригоден и достаточно точен для определения MET.

Ключевые слова: спектроскопия, ультраследовые концентрации, метформин, наночастицы золота, поверхностный плазмонный резонанс, реальные образцы.

Introduction. In recent years, researchers have paid much attention to the presence of drugs in aquatic environments and have done a lot of experiments in this area. After the consumption of pharmaceuticals, the body of humans and animals metabolizes only part of them. Then the excretion of both metabolized and nonmetabolized substances occurs. Afterwards, the final destination of these drugs will be aquatic systems [1, 2]. Due to the stability and partial degradation of these compounds, the levels of pharmaceutically active compounds (PhACs) have increased from ng/L to $\mu\text{g/L}$ levels, where they reach drinking water sources [3]. Allergy, cancer, reproductive disruption, genetic problems, and antibiotic resistance initiation in human pathogens are disadvantages of long-term exposure to diverse PhACs [4]. Therefore, measuring these contaminants in aqueous media is essential. Several methods have been developed to estimate different drugs in aqueous samples such as liquid-liquid microextraction (LLME) [5], liquid chromatography tandem mass spectrometry (LC-MS/MS) [6], colorimetry [7], fluorometry [8], micro-liquid chromatography tandem mass spectrometry [9], high-performance liquid chromatography (HPLC) [10], online solid phase extraction coupled to liquid chromatography-triple quadrupole tandem mass spectrometry (SPE-LC-MS/MS) [11], and spectrofluorimetry [12]. Among these methods, colorimetry is simple, rapid, available, and cost-effective. This technique is based on determining the concentration of the desired component by measuring the absorption wavelength [13]. Also, gold nanoparticles (AuNPs) are effective in colorimetric researches because of their excellent optical properties and high extinction coefficients [14, 15]. Localized surface plasmon resonance (LSPR), as a well-known optical aspect of AuNPs, causes color changes of AuNPs from red to blue, related to their dispersion and aggregation states, respectively [16]. One of the most abundant drugs, which still exists in wastewater treatment plant (WWTP) effluents and surface waters, is metformin (MET) (N,N-dimethylimidodicarbonimidic diamide hydrochloride) [17]:



Metformin

It is an oral antidiabetic drug and prescribed for type 2 diabetes. About 360 million people in the worldwide are diabetic. So, MET is one of the most prescribed drugs. There is a correlation between metformin consumption and its release in surface water [18]. The discharging of WWTPs containing MET into the aquatic systems can affect the food chain. Various concentrations of MET have been reported in WWTP in Canada, USA, Belgium, Portugal, Germany, and The Netherlands [19, 20]. In this study, AuNPs was synthesized by the Turkevich method [21]. AuNPs, through ligand exchange with negatively charged citrate ions, can interact strongly with positively charged amine groups of the MET. Hence, aggregation in AuNPs solution occurs, and measurement of trace amounts of MET is possible [22]. Thens spectrophotometric methods based on AuNPs were used to determine MET in drinking water. Also, determination of MET was reviewed in tablet, human serum, and urine. It was possible to determine trace amounts of MET using AuNPs without the need for a preconcentration step in the visible region. Also, the measurable concentration range was improved, and amounts up to $\mu\text{g/L}$ were easily determined by this method, which eliminates the limitation of UV-Vis spectroscopy related to the evaluation of trace amounts. For this purpose, some factors such as pH, contact time, volume and type of buffer, and ionic strength were optimized.

Experimental. Trisodium citrate dihydrate ($\text{C}_6\text{H}_5\text{Na}_3\text{O}_7 \cdot 2\text{H}_2\text{O}$), oxalic acid, sodium dihydrogen phosphate (NaH_2PO_4), sodium acetate ($\text{Na}_3\text{C}_6\text{H}_5\text{O}_7$), lead(II) nitrate ($\text{Pb}(\text{NO}_3)_2$), silver nitrate (AgNO_3), tin(II) nitrate ($\text{Pb}(\text{NO}_3)_2$), magnesium nitrate ($\text{Mg}(\text{NO}_3)_2$), iron(II) sulfate (FeSO_4), copper(II) sulfate (CuSO_4), aluminum chloride (AlCl_3), barium chloride (BaCl_2), sodium chloride (NaCl), calcium chloride (CaCl_2), and zinc chloride (ZnCl_2) were purchased from Merck. Tetrachloroauric(III) acid trihydrate ($\text{HAuCl}_4 \cdot 3\text{H}_2\text{O}$) was purchased from LOBA Chemie. Also, pure metformin hydrochloride with 99.8% purity and metformin tablets were prepared from Osvah Pharmaceutical Co.

Philips transmission electron microscopy (TEM) (CM120, The Netherlands) and MALVERN dynamic light scattering (DLS) (ZEN3600, England) were used to characterize the morphology of AuNPs and determine particle size in the nanometer range in solution, respectively. A Varian Cary 100 UV-Vis spectrophotometer was utilized to study absorptions. FTIR spectra of samples were determined using Thermo

(AVATAR, USA). METTLER TOLEDO 827 pH lab was applied to adjust pH of solutions. Also, HERMLE centrifuge (Germany, Z206A) and EYELA ultrasonic cleaner (Japan) were used.

Synthesis of AuNPs. A 0.02 g sample of HAuCl_4 was stirred in 100 mL distilled water and heated at the same time. After boiling for 2 to 5 times, 1 mL sodium citrate 1% (W/V) was added to the solution each time. The color of the solution changed from yellow to gray and immediately to wine-red, which indicates the presence of gold nanoparticles. Stirring and boiling was continued for 10 min. Then, the AuNPs were cooled at room temperature and stored in a dark bottle at 4°C .

Preparation of real samples. First, 10 tablets of MET were powdered, and part of the powder was dissolved in distilled water. Then it was transferred into a 50 mL volumetric flask and adjusted to the mark. Afterward, the solution was placed in an ultrasonic bath for 20 min and centrifuged at 4000 rpm for 10 min. The solution was transferred to a 250 mL volumetric flask and adjusted to the mark with distilled water. A specific amount of this solution was added to the AuNPs, and its absorption was recorded under optimum conditions. In the second step, the human blood serum sample of a metformin consumer was centrifuged at 4000 rpm for 20 min, the solution was transferred to a 10 mL volumetric flask, and AuNPs were added to it and its absorption measured. Finally, different concentrations of MET were added to the drinking water and urine of a person with diabetes without preparation; then AuNPs were added and their absorption recorded.

Results and discussion. Spectral characteristics. Due to the LSPR property, the color of AuNPs was red. As shown in Fig. 1a, the UV-Vis absorption of AuNPs was observed at 520 nm. After adding MET, due to the aggregation of AuNPs, the solution changed to blue, and its spectrum was found at 650 nm.

TEM, DLS, and FTIR analysis. Figures 1b,c show the TEM analysis before and after adding MET, respectively. In the absence of MET, AuNPs are dispersed. In the presence of MET, nanoparticles were aggregated together and the particle size becomes large. Also, DLS spectra of the solutions related to the absence and presence of MET are demonstrated in Figs. 1d, e. These figures indicate that the size distribution of nanoparticles in the presence and absence of MET was 10 and larger than 100 nm, respectively. Figure 2 shows the FTIR spectra of AuNPs, MET, and AuNPs in the presence of MET. The IR spectra were measured in the range of 500 to 4000 cm^{-1} . The peak at 3433 cm^{-1} in Fig. 2a is related to the OH group. Also, the peaks at 2927 and 1730 cm^{-1} are assigned to the C–H of alkane and C=O of ketone, respectively. In addition, the two bands at 1392 and 1640 cm^{-1} are attributed to the symmetric and asymmetric stretching vibrations of C=O of carboxylate. The strong bending vibration of RC(=O)R' (ketone) was evident at 1089 cm^{-1} . In the FTIR spectra of MET (Fig. 2b), the symmetric and asymmetric stretching vibrations of N–H (primary and secondary amine) were observed at 3296 and 3375 cm^{-1} , respectively. Furthermore, the strong stretching vibration at 3158 cm^{-1} is related to alkane (C–H). Also, the bending vibrations of alkene (C–H) were evident

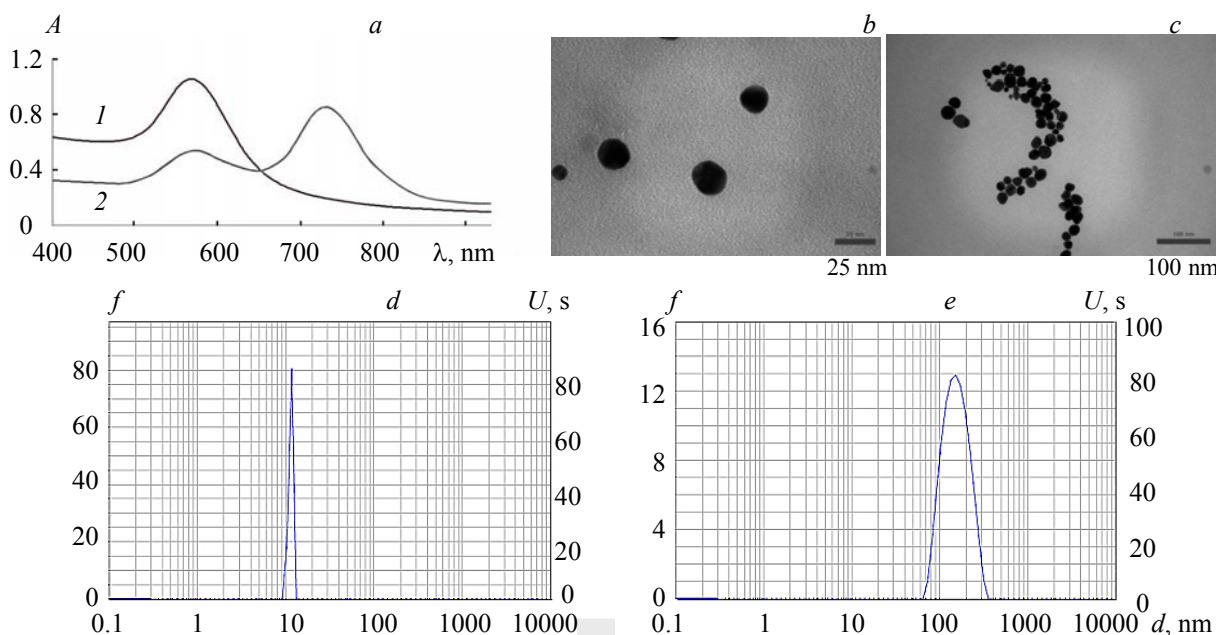


Fig. 1. UV-Vis spectra of AuNPs in the absence (1) and presence (2) of MET (a); TEM of AuNPs (b) and AuNPs+MET (c); DLS measurement in the absence (d) and presence of MET (e).

at 1449 and 1479 cm^{-1} . The stretching vibrations at 1631 and 1063 cm^{-1} was assigned to the C=N and C–N, respectively. In Figure 2c the peak of OH group was observed in the region of 3430 cm^{-1} . The strong stretching vibrations at 2925 and 2858 cm^{-1} was related to alkane (C–H). Also, the bending vibration of alkane (C–H) was evident at 1422 cm^{-1} . Amides have broad absorption in the region of 1630–1680 cm^{-1} . The C=O band interferes slightly with the bending vibration of N–H at 1640–1560 cm^{-1} . So, the C=O is shown as a twin branch. The amide group represents the interaction between MET and the AuNPs covered with citrate. The location of absorption bands in the spectrum (a) does not show a significant displacement relative to the spectrum (c). The location of the absorption bands of MET in the spectrum (c) is slightly displaced relative to the location of its absorption bands in the spectrum (b). The drug interacts with citrate, which causes bond change and vibrational frequency change. Therefore, the absorption bands are slightly displaced [16, 23].

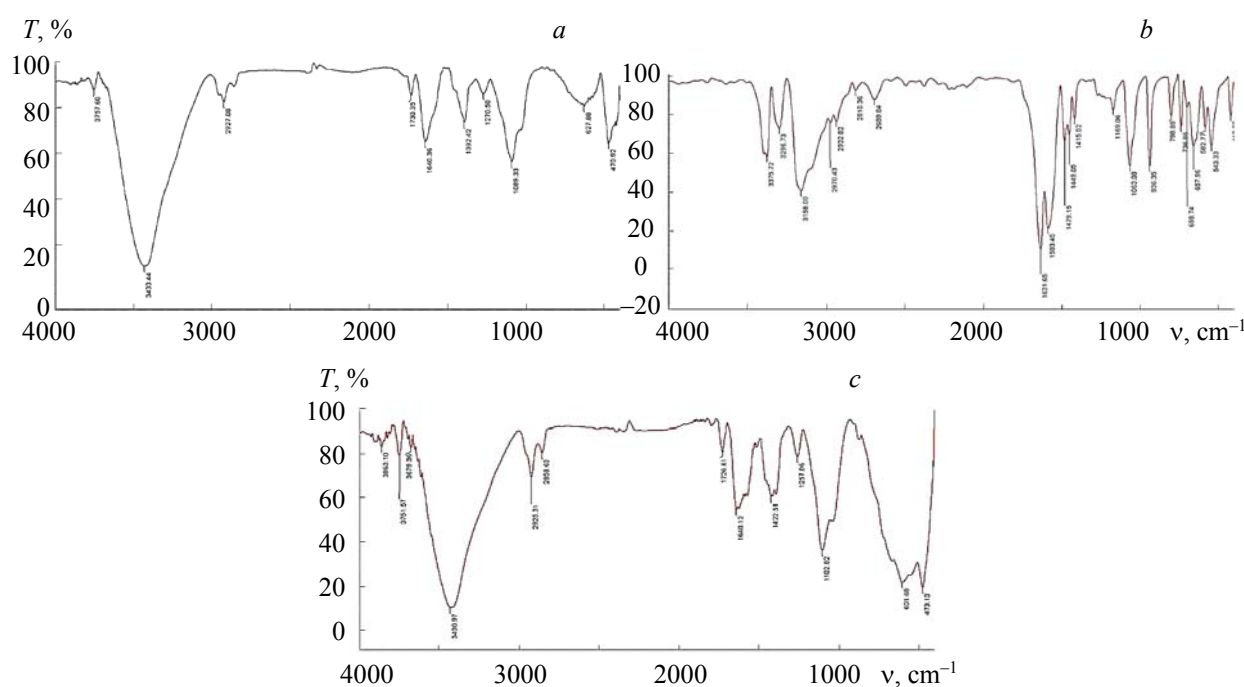


Fig. 2. FTIR spectra of AuNPs (a), MET (b), and AuNPs+MET (c).

Optimization of parameters. The effect of pH in the range of 2–12 was studied for selecting optimal conditions. The pH of solutions was adjusted by HCl and NaOH. As shown in Fig. 3a, the relative intensity of absorption increased gradually with increasing pH, and the maximum absorption was obtained at pH 6.5. Due to the deprotonation of the amine group in pH 6.5, the bond between the AuNPs and MET was strengthened, and the aggregation of gold nanoparticles and surface plasmon resonance in the presence of the drug was improved. Aggregation does not occur or is very small at higher and lower pH. So, the best pH is 6.5. Due to the importance of AuNPs concentration in the sensitivity of the proposed method, the effect of AuNPs concentration was evaluated. So, various amounts of AuNPs solution (0.05–48.4 nmol/L) were prepared to survey the absorption spectra. Also, different times were investigated for finding the optimal value. Figure 3c shows that AuNPs began to aggregate after mixing with MET, and spectral changes can be seen at 8 min. After 8 min, time does not have an effect on absorption. In addition, the effect of oxalate, phosphate, and acetate buffers was investigated on the absorption of AuNPs for determination of metformin. Figure 3d shows that the phosphate buffer has the highest absorption, so, it is selected as the optimum buffer. Then different volumes of phosphate buffer (100–1000 μL) were tested to select the optimal buffer volume. It can be concluded from Fig. 3e that 100 μL was the best volume for measuring MET. Furthermore, ionic strength plays a key role in the process of aggregation. Hence, different concentrations of NaCl were added to the solution, and the ionic strength was investigated. Increasing the NaCl concentration maintains the surface charge and reduces the distance between particles; finally, the aggregation of particles occurs. It was also found that by increasing the ionic strength to greater than a certain limit, the aggregation of nanoparticles is induced even in the absence of analyte. According to Fig. 3f, the concentration of 0.5 $\mu\text{g/L}$ was chosen as the optimum value.

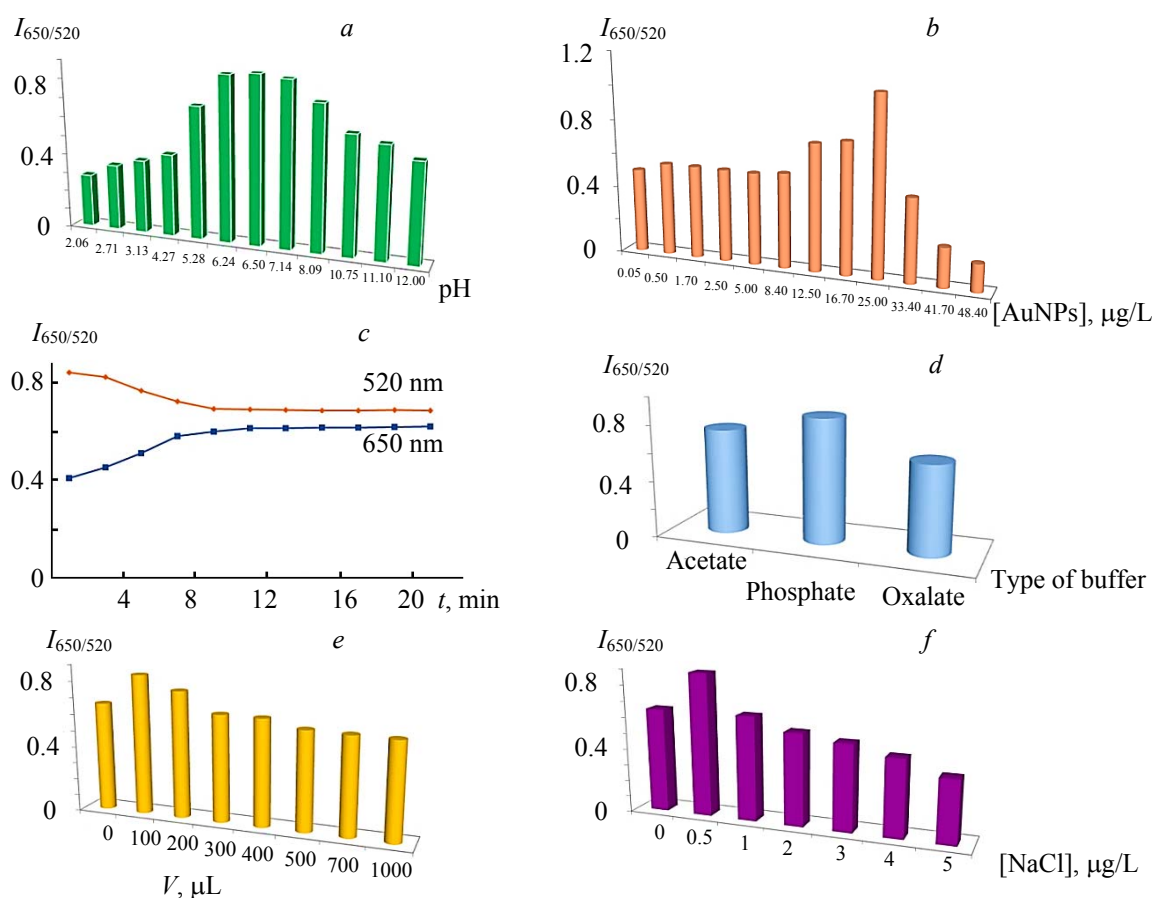


Fig. 3. The influence of pH (a), concentration of AuNPs (b), time (c), type of buffer (d), volume of buffer (e), and concentration of NaCl (f) on the surface plasmon intensity.

Effect of interfering substances. Under optimum conditions, salts of different metals were prepared with different concentrations. Then the amount, of nanoparticles and metal ions with concentration 1000, 100, and 10 times greater than the drug, and also the same concentration of metal ion and drug, was measured. At each stage, ions with smaller absorption difference, where their diagrams are similar to the optimal nanoparticle–MET curve, were detected as the interfering ion, and the dilution continued until the ion was removed. As shown in Table 1, the permitted concentrations of these interfering species are higher than the MET concentration, which indicates that the proposed method has good selectivity between drug and other species.

TABLE 1. Effect of Interfering Species on the Determination of MET

Interference	Tolerance limits $[X]/[MET]$
Ag^+ , Na^+	1000
Fe^{2+} , Sn^{2+} , Pb^{2+} , Cl^- , SO_4^{2-}	100
Mg^{2+} , Zn^{2+}	10

Calibration graph and detection limit. Under optimal experimental conditions, the calibration curve was plotted to determine MET. Figure 4a shows that the proposed method has good linearity in the range of 15 to 300 $\mu\text{g/L}$. The correlation coefficient (R^2) was equal to 0.9918. Also, the limit of detection (LOD) and limit of quantification (LOQ) were calculated using the formulas $\text{LOD} = y_B + 3s_B$ and $\text{LOQ} = y_B + 10s_B$, respectively, where y_B is the intercept of the regression line and s_B is the standard deviation of the blank signal [24]. The LOD and LOQ obtained were 0.990 and 1.120 $\mu\text{g/L}$, respectively. The results indicate that this method has a high ability to measure MET.

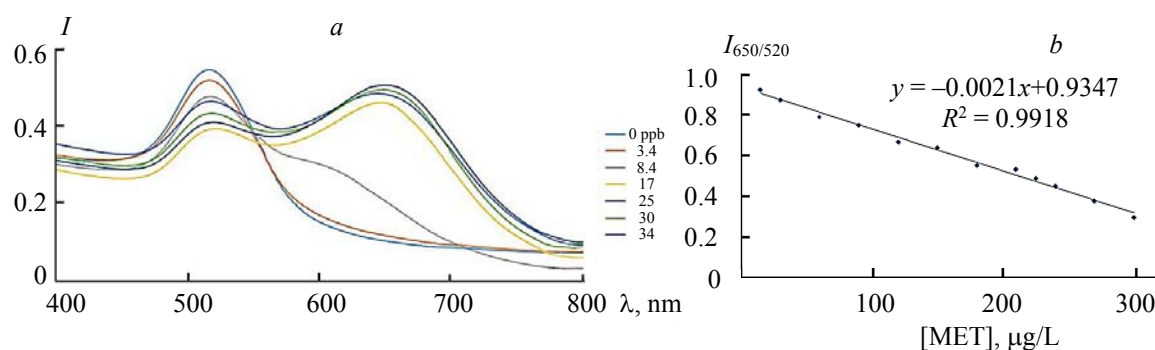


Fig. 4. Overlaid UV-Vis spectra of AuNPs–MET (a) and calibration graph for determination of MET (b).

Analysis of real samples. In order to evaluate the applicability and validity of this method, real samples, including drinking water, tablet, human serum, and urine were used to determine MET. These samples were spiked with various concentrations of MET, and the influence of the matrix was estimated. The results in Table 2 show that recoveries are good for determination of MET.

TABLE 2. Determination of MET in Real Samples ($n = 3$)

Sample	Added MET, $\mu\text{g/L}$	Found MET, $\mu\text{g/L}$	Recovery, %	RSD, %
Tablet	0	3.95	–	0.11
	8	11.52	94.62	0.07
	16	19.52	97.31	0.09
Drinking water	0	Not detected	–	0.08
	8	8.33	104.12	0.12
	16	15.47	96.68	0.10
Human Serum	0	2.14	–	0.10
	8	9.85	96.37	0.09
	16	17.28	94.62	0.06
Urine	0	1.71	–	0.06
	8	9.57	98.25	0.08
	16	17.04	95.81	0.08

Comparison with other methods. Table 3 shows a comparison between the results of the proposed method and those for some other methods for determining the MET. As can be seen, the current method yields good LOD and LOQ, as well as an acceptable linear range compared to the previously published methods.

TABLE 3. Comparison of the Proposed Method with Some of the Previously Reported Methods for the Determination of MET

Method	Linear range, $\mu\text{g/L}$	LOD, $\mu\text{g/L}$	LOQ, $\mu\text{g/L}$	Real sample	References
HPLC	2–2000	–	1.6	Urine	[25]
UPLC	1.7–100	0.4	1.7	Plasma	[26]
GC-MS	0.01–0.05	0.004	0.0155	Surface water	[1]
RP-HPLC	0.005–0.03	0.00032	0.00099	Tablet	[27]
Spectrophotometry	15–300	0.99	1.12	Drinking water, tablet, serum, urine	Present study

Conclusions. The determination of metformin was performed using a UV-Vis spectrometer based on surface plasma resonance absorption of gold nanoparticles. Metformin can interact with AuNPs and causes the dispersion of AuNPs (red) to the aggregation form (blue). The developed method is simple, cost-

effective, sensitive, rapid, eco-friendly, and requires no expensive tools. The proposed method is promising for measuring the metformin in drinking water, tablet, serum, and urine samples. This method has broad prospects for measuring other drugs as water pollutants. As reported in various articles, it can also have applications in the medical and pharmaceutical industries.

REFERENCES

1. C. Goedecke, I. Fetting, C. Piechotta, R. Philipp, S. U. Geissen, *Anal. Methods*, **9**, 1580–1584 (2017).
2. M. Alnajjar, A. Hethnawi, G. Nafie, A. Hassan, G. Vitale, N. N. Nassar, *J. Environ. Chem. Eng.*, **7** (2019).
3. Z. Cai, A. Dhar Dwivedi, W. N. Lee, X. Zhao, W. Liu, M. Sillanpää, D. Zhao, C. H. Huang, J. Fu, *Environ. Sci. Nano*, **5**, 27–47 (2018).
4. F. I. Hai, S. Yang, M. B. Asif, *Water*, **10**, 107–139 (2018).
5. T. Macedo Rosa, A. Carolina Roveda, W. P. da Silva Godinho, C. A. Martins, P. R. Oliveiraa, M. A. Gonçalves Trindade, *Talanta*, **196**, 39–46 (2019).
6. R. Oertel, J. Baldauf, J. Rossmann, *J. Chromatogr. A*, **1556**, 73–80 (2018).
7. R. A. Khalila, A. M. A. Saeed, *J. Chin. Chem. Soc.*, **54**, 1099–1105 (2007).
8. A. Saini, J. Singh, R. Kaur, N. Singh, N. Kaur, *Sens. Actuat. B*, **209**, 524–529 (2015).
9. A. Celma, J. V. Sancho, N. Salgueiro-Gonzalez, S. Castiglioni, E. Zuccato, F. Hernandez, L. Bijlsma, *J. Chromatogr. A*, **1602**, 300–309 (2019).
10. M. Khoeini Sharifabadi, M. Saber-Tehrani, S. W. Husain, A. Mehdinia, P. Aberoomand-Azar, *Sci. World J.*, **2014**, 1–8 (2014).
11. B. Yao, L. Lian, W. Pang, D. Yin, S. A Chan, W. Song, *Chemosphere*, **160**, 208–215 (2016).
12. E. Bakir, M. Gouda, A. Alnajjar, W. E. Boraie, *Acta Pharm.*, **68**, 243–250 (2018).
13. M. H. Jazayeri, T. Aghaie, A. Avan, A. Vatankhah, M. R. S. Ghaffari, *Sens. Bio-Sens. Res.*, **20**, 1–8 (2018).
14. M. Bahram, S. Alizadeh, *Int. J. Biotech. Bioeng.*, **4**, 21–32 (2018).
15. N. Xia, D. Deng, Y. Wang, C. Fang, S. Juan Li, *Int. J. Nanomed.*, **13**, 2521–2530 (2018).
16. M. Bahram, T. Madrakian, S. Alizadeh, *J. Pharm. Anal.*, **7**, 411–416 (2017).
17. A. Leovac Macerak, D. Kerkez, M. Becelic-Tomin, D. Tomasevic Pilipovic, A. Kulic, J. Jokic, B. Dalmacija, *Proc. MDPI Publ.*, **2**, 1288–1291 (2018).
18. M. Scheurer, F. Sacher, H. Jurgen Brauch, *J. Environ. Monitor.*, **11**, 1608–1613 (2009).
19. Y. Tao, B. Chen, B. H. Zhang, Z. J. Zhu, Q. Cai, *Occur., Impact, Adv. Mar. Biol.*, **81**, 23–58 (2018).
20. M. Scheurer, A. Michel, H. Jurgen Brauch, W. Ruck, F. Sacher, *Water Res.*, **46**, 4790–4802 (2012).
21. J. Turkevich, P. Cooper Stevenson, J. Hillier, *Discuss. Faraday Soc.*, **11**, 55–75 (1951).
22. N. Shahbazi, R. Zare-Dorabei, *ACS Omega*, **4**, 17519–17526 (2019).
23. C. Senthil Kumar, M. D. Raja, D. Sathish Sundar, M. Gover Antoniraj, K. Ruckmani, *Carbohydr. Polym.*, **128**, 63–74 (2015).
24. J. N. Miller, J. C. Miller, *Statistics and Chemometrics for Analytical Chemistry*, 6th ed. (2010).
25. R. Q. Gabr, R. S. Padwal, D. R. Brocks, *J. Pharm. Pharm. Sci.*, **13**, 486–494 (2010).
26. A. M. Strugaru, J. Kazakova, E. Butnaru, I. C. Caba, M. Angel Bello-Lopez, R. Fernandez-Torres, *J. Pharm. Biomed. Anal.*, **165**, 276–283 (2019).
27. M. Tgk, J. Geethanjali, *J. Chromatogr. Sep. Technol.*, **5**, 252–259 (2014).